

# Modelling the reinforced concrete beams strengthened with GFRP against shear crack

Mustafa Kaya\* and Canberk Yaman

Faculty of Engineering, Aksaray University, Aksaray, Turkey

(Received March 14, 2017, Revised June 6, 2017, Accepted September 28, 2017)

**Abstract.** In this study, the behavior of the number of anchorage bolts on the glass-fiber reinforced polymer (GFRP) plates adhered to the surfaces of reinforcing concrete (RC) T-beams was investigated analytically. The analytical results were compared to the test results in term of shear strength, and midpoint displacement of the beam. The modelling of the beams was conducted in ABAQUS/CAE finite element software. The Concrete Damaged Plasticity (CDP) model was used for concrete material modeling, and Classical Metal Plasticity (CMP) model was used for reinforcement material modelling. Model-1 was the reference specimen with enough sufficient shear reinforcement, and Model-2 was the reference specimen having low shear reinforcement. Model-3, Model-4 and Model-5 were the specimens with lower shear reinforcement. These models consist of a single variable which was the number of anchorage bolts implemented to the GFRP plates. The anchorage bolts of 2, 3, and 4 were mutually mounted on each GFRP plates through the beam surfaces for Model-3, Model-4, and Model-5, respectively. It was found that Model-1, Model-3, Model-4 and Model-5 provided results approximately equal to the test results. The results show that the shear strength of the beams increased with increasing of anchorage numbers. While close results were obtained for Model-1, Model-3, Model-4 and Model-5, in Model-2, the rate of increase of displacement was higher than the increase of load rate. It was seen, finite element based ABAQUS program is inadequate in the modeling of the reinforced concrete specimens under shear force.

**Keywords:** Finite Element Method; nonlinear analysis; shear strengthening; GFRP; anchorage

## 1. Introduction

Reinforced concrete shows heterogeneous, isotropic, non-elastic, and time-dependent material behavior. Laboratory tests, numerical methods, computer and model analyses are studies for us to have more information about the nonlinear behavior of reinforced concrete.

The behavior of the structure with computer modelling can be observed more economical, and faster than experimental studies and numerical analysis. If appropriate, the necessary changes can be made easily and quickly to have knowledge on different parameters.

Nonlinear behavior of structural elements was analyzed by developed computer models. Many models were created in the past for nonlinear analysis, and the same model analysis results were compared with test results.

Helba *et al.* (1995), investigated the ultimate collapse loads of composite steel bridges by using the yield line method and FEA performed using ABAQUS. Only limited information on the FEA was available. However, no load-deflection relationships were available to show the ability of the FEA to capture the load-deflection characteristics.

Thevendran *et al.* (1991), studied the ultimate load-carrying capacity of simply supported composite steel beams curved in plan by using ABAQUS. The slab was

modeled by 4-node isoparametric thick shell elements, while girders were modeled by 4-node isoparametric thin shell elements. Rigid beam elements were used to model shear connectors. Nonlinear material properties were included. No information was provided to describe the concrete reinforcement, which is critical in the FEA of continuous span composite steel bridges FEA deviated greatly from the experimental results, particularly in the nonlinear regions and FEA did not capture the complete load-deflection characteristics and the ultimate strength initial cracking. Ahmed (2014), recommended a 3D finite element (FE) analysis technique using ABAQUS was chosen to explore the dynamic behavior of a beam under impact load. A beam, was selected to develop a solid FE model. FE analyses were performed implementing ABAQUS Explicit programming tool to predict the dynamic responses under the pressure amplitude. Thirty analyses have been executed, changing different parameters, such as dumping, tension and compression stiffness recovery, damage parameter, strain/displacement relations and friction coefficient to choose the best performing FE analysis model. The high accuracy definition was confirmed upon extensive examination of the calculated structural responses of the FE model compared with the test results. Baska *et al.* (2002), developed 3D FEA models using ABAQUS to carry out the nonlinear analysis of composite steel plate girders under negative bending and shear loading. Various methods were proposed to model the concrete behavior and composite action characteristics. Various elements were selected in the analyses. Previous

---

\*Corresponding author, Associate Professor  
E-mail: [kaya261174@hotmail.com](mailto:kaya261174@hotmail.com)

experimental data from other researchers were used to examine the accuracy of the modeling techniques. This revealed that (1) the surface interaction method suggested for modeling composite action was not capable of carrying out the analysis to failure, and (2) the cast iron and metal elastic-plastic models were not realistic for modeling concrete. A comparison of the load-deflection behavior of the experimental and analytical results indicated poor agreement, in both linear and nonlinear regions. Different tension models have been used in the FEA for RC structures (Gilbert and Warner 1990, Gupta and Maestrini 1990). Four different concrete tensile stress-strain curves were summarized: brittle without tension stiffening, stepped response after cracking, gradual unloading after cracking and discontinuous unloading after cracking. The third, gradual unloading after cracking, is the closest to the actual concrete cracking behavior. A generalizations are made by Dogan (2010), on effective bonding length by increasing the amount of test data. For this purpose, ANSYS software is employed, and an experimentally verified nonlinear finite element model is prepared. Special contact elements are utilized along the concrete-CFRP strip interface for investigating stress distribution, load-displacement behavior, and effective bonding length. Then the results are compared with the test results. The finite element model found consistent results with the experimental findings. Demir *et al.* (2016) proposed a new shear reinforcement configuration named as diagonal shear reinforcement (DSR). For this objective a numerical nonlinear finite element (FE) study is performed by considering two tested beams with flexural and shear failure modes. These two test results are first verified numerically then DSR is included in existing FE model to start a parametric study for highlighting the efficiency of proposed DSR shear reinforcement configuration. The numerical results demonstrate that there is a significant increase in shear and ductility capacity of RC beams when proposed DSR is included. Moreover, with an increase in diameter and yield strength of DSR, the shear capacity further improves and failure mechanism shifts from shear to flexure.

Stramandinoli (2012), a finite element (FE) model for nonlinear analysis of reinforced concrete (RC) beams, considering shear deformation, is developed. The Fiber Model is adopted, with the element section discretized into overlaid concrete and longitudinal reinforcement layers. Transverse reinforcement, when present, is considered to be smeared and embedded in the concrete layers. In Kmiecik and Kaminski (2011), study parameters are illustrated using the Concrete Damaged Plasticity model included in the ABAQUS software.

Ibrahimbegovic *et al.* (2010), present a novel approach to the finite element modelling of *reinforced-concrete* (RC) structures that provides the details of the constitutive behavior of each constituent (concrete, steel and bond-slip), while keeping formally the same appearance as the classical finite element model. Mahmud *et al.* (2013) studied on Ultra High Performance Steel Fiber Reinforced Concrete (UHPRFC). The size effects on the structural strength of UHPRFC members remain largely unknown. This is mainly due to the lack of sufficient and reliable test data. This study

investigates the size effects on the flexural strength of similar notched UHPRFC beams under three-point bending tests. Nonlinear finite element simulations using the concrete damage plasticity (CDP) model in ABAQUS were also conducted, using material properties extracted from uniaxial tensile and compressive laboratory tests. It was found that the size effect on the beam nominal strength is less due to high ductility of UHPRFC. The numerical simulations using the CDP model can predict load-displacement curves and crack propagation process with good agreement with test data. Zivaljic *et al.* (2014), reviewed several computational aspects of the combined finite element method related to the modelling of plane reinforced concrete progressive fracturing. It discusses especially the ability of the presented numerical model, extended with a new model of reinforcing bar, to simulate the behavior of the reinforced concrete structure through the entire failure mechanism from the continuum to the discontinuum. Larbi *et al.* (2013) experimental and numerical study is related to the repair and strengthening of reinforced concrete beams with TRC (textile-reinforced concrete) and hybrid (TRC+carbon and glass rods) solutions that are positioned relative to the more traditional ones such as the CFRP (carbon fiber-reinforced polymer) solutions. Beyond the good performances highlighted experimentally, especially in terms of bearing capacity and different failure modes (e.g., possibility to avoid peeling off), it is clear from this work that the TRC, despite its nonlinear behavior (multi-cracking), does not allow a significant gain in ductility. Numerical modelling performed on all the beams also highlighted the fact that the axial stiffness of reinforcements (even in the case of a cracking material) governing the overall behavior of beams could, at least in part, explain the observed failure modes. In the Xu *et al.* (2015), investigation, shear transfer behavior in initially uncracked reinforced concrete members is conducted using finite element modeling method. One of the aims of this study is to improve insight into the characteristics between the shear stress and slip for a range of design parameters. The other aim of this study is to derive a set of simplified equations for evaluating the ultimate shear stress and relationship of shear stress to slip in practical structural design. Parametric studies are then carried out to generate data with the consideration of different combinations of the structural design parameters, i.e., concrete strength, percentage of dowel steel and lateral normal pressures. It is found that the numerical models are accurate in predicting the interface shear strength and slip occurring along the shear plane of the push-off test specimens. Lee *et al.* (2014), introduced the direct tension force transfer model, in which tensile resistance of the fibers at the crack interface can be easily estimated, to the nonlinear finite element analysis algorithm with the fixed-angle theory, and the proposed model was also verified by comparing the analysis results to the shear panel test results. The secant modulus method adopted in this study for iterative calculations in nonlinear finite element analysis showed highly stable and fast convergence capability when it was applied to the fixed-angle theory. Domínguez *et al.* (2015), prepared different nonlinear finite element models

for eight simply supported reinforced concrete haunched beams designed to develop a shear failure under static loading. Nonlinear finite element models were assessed with ANSYS, in which longitudinal steel reinforcement and stirrups were modeled as built. Softening of concrete due to deformation was taken into account in the selected constitutive models using a failure surface with different peak compressive and tensile stresses. Strain hardening for the steel reinforcement was considered using the Von Mises yield criterion. The perfect bond between concrete and steel was assumed. Shear-displacement curves for a specific section located at midspan of the beams were obtained from the finite element models and compared to those obtained from experimental testing. Also, crack patterns associated with different load steps were obtained from ANSYS finite element model. Nistico *et al.* (2016), strengthened reinforced concrete (RC) beams strengthened in shear with Carbon Fiber Reinforced Polymer (CFRP). The aim is to validate a numerical approach, which is based on the microplane model for concrete and polymer (matrix), and to better understand the stress distribution in CFRP when the concrete crack initiates and propagates. The numerical study is supported by results of experimental tests, regarding 10 beams reinforced with different technological solutions in terms of strength and ductility. The study focused on the analysis of two RC beams, the first without FRP and the second completely wrapped with CFRP. The numerical 3D finite element (FE) analysis is carried out using the FE code that is based on the microplane model for concrete and FRP. Ruano *et al.* (2015), improved tensile properties of steel fiber reinforced concrete (SFRC) make it suitable for repairing and strengthening of reinforced concrete elements. The numerical simulation of the mechanical behavior of a series of reinforced concrete beams which includes strengthening and repaired beams with high performance self compacting SFRC tested under shear. An evolutionary algorithm is proposed in order to simulate the whole process of testing, repairing and retesting the beams. The numerical simulations can accurately reproduce flexure characterization tests and predict the bearing capacity of the repaired and

strengthened beams tested under shear. Furthermore, other repairing/strengthening options are numerically studied. The numerical results could be useful to improve the design of this kind of intervention techniques. Silva (2016), reports on a set of numerical simulations for the investigation of the shear strength of exterior joints. The geometry of the joints and the stress level of the column is the variables evaluated. The results have led to empirical expressions that provide the shear strength of unreinforced exterior beam-column connections. Kotsovou (2016), concerned with a numerical investigation of the behavior of reinforced-concrete beams with non-bonded flexural tension reinforcement. The numerically-established behavior of such beams with and without transverse reinforcement is compared with its counterpart of similar beams with bonded reinforcement. Solomon *et al.* (2010), Investigated experimentally and numerically the behavior of RC beams strengthened in flexure with NSM-FRP bars. A total of twenty reinforced concrete beams were constructed and tested till failure. Test results showed that the use of NSM-FRP bars are effective in increasing the flexural capacity of concrete beams. Comparisons between the FE predictions and test results showed very good agreement in terms of the load-deflection and load-strain relationships, ultimate capacities, and modes of failure for the tested beams. Hawileh (2012), presented a development of a detailed 3D nonlinear FE model that can accurately predict the load carrying capacity and response of RC beams strengthened with NSM-FRP rods subjected to four-point bending loading. The developed FE model considers the nonlinear constitutive material properties of concrete, yielding of steel reinforcement, cracking of the filler bonding materials, bond slip of the steel and NSM reinforcements with the adjacent concrete surfaces, and bond at the interface between the filling materials and concrete. The numerical FE simulations were compared with test, measurement tested by other investigators comprising of seven specimens strengthened with NSM CFRP rods in addition to one un-strengthened control specimen. In the Yaman (2015) study, the effect of the number of anchors on the shear strength of beams was analytically investigated. In this direction, reinforced

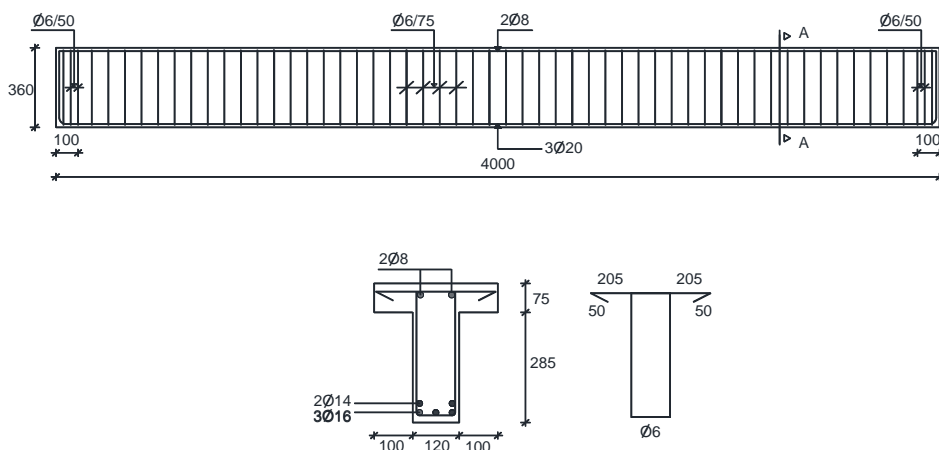


Fig. 1 DE1 sufficient reference test specimen

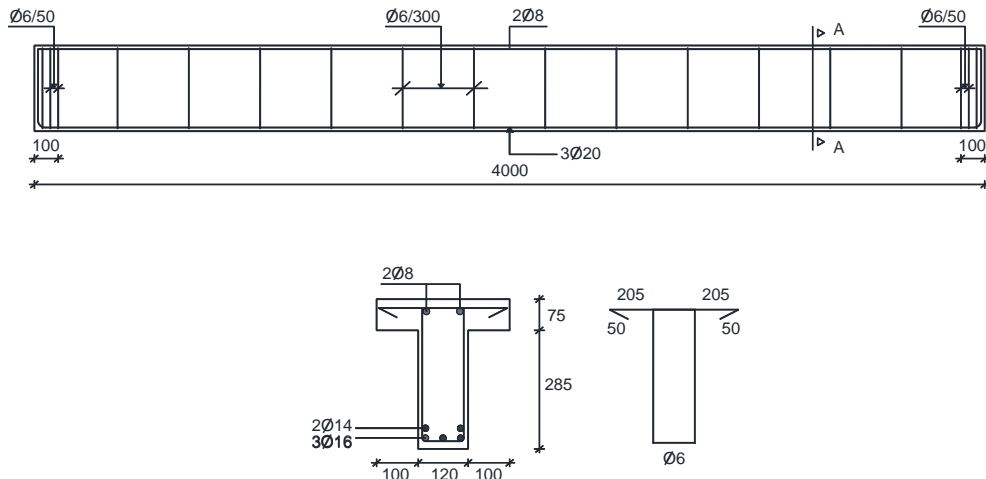


Fig. 2 DE2 insufficient reference test specimen

concrete beams were modeled with the ABAQUS finite element program. Concrete Damaged Plasticity concrete damage model and Classical Metal Plasticity model were used. Then, nonlinear analysis of these models was done. The results obtained from previous experiments were compared with the analysis results.

## 2. Experimental study

### 2.1 Description of test specimens and test setup

In the study, 1 sufficient reference specimen (Fig. 1), and 4 insufficient shear reinforcement insufficient reference specimen (Fig. 2) were produced shear reinforcement insufficient specimens according to the Regulation on buildings to be built in earthquake regions (DBYBHY 2007). 4 shear reinforcement insufficient specimens stirrup ratio was  $\rho_w=0.00157$  (Fig. 1). The length of the T-shaped beam was 4000 mm. The flange of the beam has 320 mm width, and 75 mm thick. The web of the beam has of 120 mm width, and 360 mm depth. The concrete compressive strength employed in the specimen was 16 Mpa. The diameter of the stirrup was 6 mm. The spacing of the stirrup was 75 mm for a specimen with shear reinforcement sufficient beam, the spacing of the specimen with shear reinforcement insufficient beam (Model-1, and Model-2). The bottom longitudinal bars were arranged in two layers, the first layer has three bars of 16 mm diameter, and the second layer has two bars of 14 mm diameter. The top longitudinal bars have two bars of 8 mm diameter.

In the study, the effect of the number of anchorages on the shear strength of the beams was investigated. For all the specimens the beam section was the same, GFRP has ( $W_f$ ) 90 mm width, 280 mm height and 5 mm thick. GFRP strips affixed to the beams side face mutually with epoxy in 3 specimens which were strengthened (Fig. 3). The axis range of the CFRP strip which was glued to the beam side surface was selected to be 100 mm. Anchoring was applied to all strengthened elements. Anchorages provide better adhesion of GFRP strips to the beam surface. In the strengthened

Table 1 Concrete specimens average compressive strengths

Specimen number	Concrete compressive Strength (MPa)
1	15,8
2	16,0
3	16,2
4	15,9
5	16,4
6	16,1

specimens, the anchorage range was applied at 180 mm for 2 anchored elements, 90 mm for 3 anchored elements, and 60 mm for 4 anchored elements. All beams in operation were tested under monotonic loads.

### 2.2 Installation program

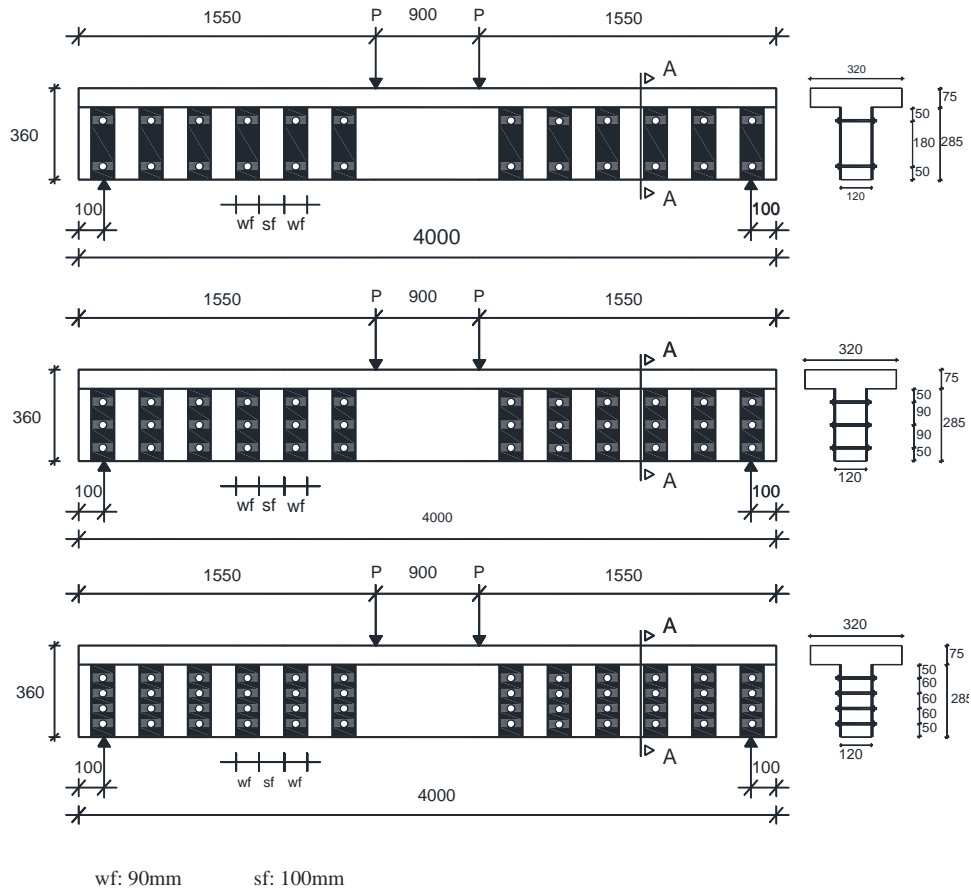
The load was applied to the test specimens by means of mechanical pump connected to hydraulic jack. The intensity of the load was measured with a load cell. The test specimens were placed on the simple supports. The applied load (P) from the hydraulic jack was transmitted to the test specimens by reaction beam places at the center of the specimen. Electronic measurement devices (LVDT) were placed at mid-span of the beam, left, and right support the beam in order to record the midpoint displacement of test specimens (Fig. 4). The three LVDTs measured the mid-span displacement, left and right support displacements.

### 2.3 Material

In order for the results of the experimental study to be compared correctly, the test specimens must be produced from the same characteristic material. For this purpose, the same characteristic feature was used in the experimental study.

#### 2.3.1 Concrete

C16 concrete was used in the production of the test specimens. The average compressive strength of concrete samples obtained from the 28-day test were given in Table 1.



wf: 90mm sf: 100mm

$s_j$ : Distance between GFRPs;  $w_j$ : Width of GFRP

Fig. 3 DE3, DE4 and DE5 strengthened test specimens

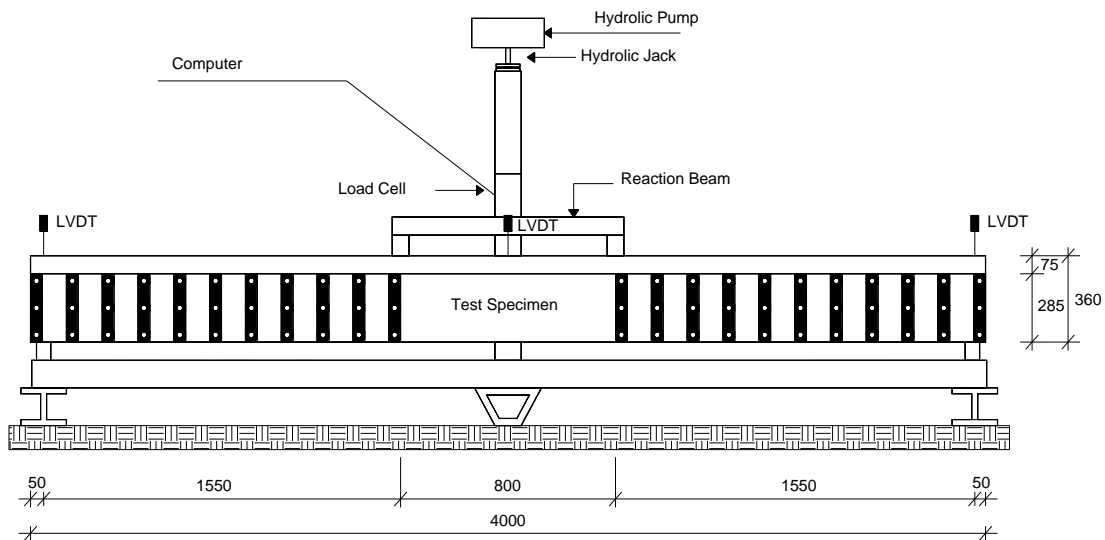


Fig. 4 Test setup and measurement system

The concrete strength determined in the production of the test specimens is the average compressive strength of the concretes of the damaged structures in the Marmara earthquake that took place in 2009 in our country.

### 2.3.2 Reinforcement

The properties of the reinforcement used in the test

specimens were given in Table 2.

### 2.3.3 GFRP

Glass fiber reinforced polymer was used in this work because it is cheap and easily accessible. Although the glass fibers aren't as light and rigid as carbon fibers, they are very cheap strengthening materials. The properties of GFRP used

Table 2 Yielding and tensile strengths of the mild steel used in the experiments

Reinforcement diameter	Steel class	Yielding Stress (MPa)	Fracture stress (MPa)
Ø 6	S220	390	630
Ø 8	S420	440	670
Ø 14	S420	450	680
Ø 16	S420	470	695

Table 3 Properties of GFRP

Unit weight (gr/cm <sup>3</sup> )	1.5-2.1
Tensile strength (MPa)	200-340
Impact strength (MPa)	33
Modulus of elasticity (N/mm <sup>2</sup> ): 260000	

in the test specimens were given in Table 3.

#### 2.3.4 Structural adhesive

Sikadur 31 used to attach GFRP strip to the beam surface. Sikadur 31 2-component, epoxy resins and special fillings containing structural bonding, and repair mortar. The mechanical/physical properties of epoxy adhesives were given in Table 4.

#### 2.4 Experimental test results

The reference test specimen with sufficient shear reinforcement (DE1) was to which strengthening was not applied. The load capacity of this specimen was 185,96 kN. The mid-span displacement of the specimen measured at the collapse was 56,08 mm. This test specimen exhibited ductile behavior. The collapse of the specimen results from the yielding of bending reinforcement. The specimen without sufficient shear reinforcement (DE2) has the load capacity of 138,76 kN. The displacement at maximum load was 22,07 mm. This specimen collapsed as a result of shear cracking. DE3 specimen consisting of 2 anchorage bolts applied to GFRP plates carried the load of 169,8 kN. The mid-span displacement of this specimen measured at the collapse was 28,23 mm. This specimen collapsed suddenly in a brittle way as a result of shear cracking. DE4 specimen having 3 anchorage bolts applied to GFRP plates carried the load 174,94 kN. The mid-span displacement was 28,45 mm. This specimen was fractured suddenly in a brittle manner as a result of shear cracking. DE5 specimen which consists of 4 anchorage bolts applied to GFRP plates has the load capacity of 185,30 kN. The mid-span displacement of this specimen was 44,98 mm. This specimen carried the load approximately equal to the load of DE1 sufficient reference specimen. This test specimen exhibited ductile behavior and collapsed as a result of yielding of bending reinforcement.

Strengthened DE2 and DE3 specimens collapsed because of shear fracture. While testing these specimens their bending reinforcements did not yield, and these specimens collapsed at the lowest displacements. But, strengthened DE5 specimen collapsed because of yielding of the bending reinforcement. As a result this specimen collapsed at the highest displacement.

Table 4 Sikadur 31 epoxy mechanical and physical properties

	Cure duration	Cure temperature	
		+20 C°	+10 C°
Compressive strength	1 days	40-45 N/mm <sup>2</sup>	35-40 N/mm <sup>2</sup>
	10 days	60-70 N/mm <sup>2</sup>	50-60 N/mm <sup>2</sup>
	Cure duration	Cure temperature	
		+10 C° ~ +20 C°	
Flexural strength	10 days	30-40 N/mm <sup>2</sup>	
Tensile strength	10 days	15-20 N/mm <sup>2</sup>	
Adhesion strength	10 days	3,0-3,5 N/mm <sup>2</sup>	
	10 days (steel)	15 N/mm <sup>2</sup>	
Modulus of elasticity		4300 N/mm <sup>2</sup>	
Density		1,65 kg/l	

The load capacity of specimens increased with the increasing of the number of anchorage bolts applied to GFRP plates.

### 3. Nonlinear behavior

#### 3.1 Impact of nonlinear behavior in buildings

Reinforced concrete elements may only behave linearly under the influence of low loads, ie. service loads. Time-dependent effects, or environmental conditions such as temperature, corrosion, friction, shrinkage, etc. affect the behavior of the concrete. Because of the effects on reinforced concrete elements, time-dependent cracks were formed and cracks may develop. For this reason, the real behavior of reinforced concrete elements can be modeled by nonlinear analysis.

The general principle of nonlinear analysis is load applying to the specimen step by step. Each step is approached to the actual behavior by influencing the results of the previous step. In the analysis of the structure in this way, deformations, displacements and changes in stiffness are not neglected.

There are some reasons for the nonlinear behavior of building elements. These; Geometric nonlinearity, and material nonlinearity. Displacements that occur in the element, or structure is related to geometric nonlinearity. Material nonlinearity can be explained as a linear feature of materials used in building elements.

Various studies are still being carried out to understand the nonlinear behavior of the structures. Laboratory experiments, numerical methods, and model analyzes are studied to gain more knowledge about the nonlinear behavior of concrete. Computer modelling does not bring as much time, and cost as experimental studies. In addition, parameters that were effective in the analysis can be changed in the short time to allow for different studies.

#### 3.2 Nonlinear solution methods

The stiffness of the system changes depending on the

displacement of nonlinear behavior materials. The method used in this model is a sequential approach. In this method, the displacements are linearized with the previous values. Other methods used in calculations are initial tangent, initial beam, and tangent method (Bath and Wu, 2006). In the initial tangent method, the calculations are done linearly at each step. The stiffness matrix (matrix of coefficients) is the same in every step. In the initial beam, beam and tangent methods, the matrix of coefficients is different in each step. The difference between these methods was the level of convergence speed.

#### 4. Finite element method

##### 4.1 Definitions of the finite element method

The finite element method allows us to achieve results that are closer to the truth by allowing nonlinear analysis solutions. They do not bring as much time and cost as the experimental study. Despite numerical methods, results can be obtained much sooner. In addition, the parameters that are effective in the analysis are changed in a short time, allowing for different research. However, if the material properties and geometry cannot be properly identified, the results are deviating from their actual results. The basic principle in the finite element method is that the object to be solved is divided into several simple, smaller meshes that are related to each other. In order to obtain more accurate results in the analysis, the mesh density needs to be kept high. However, too much mesh density increases the duration of analysis too much.

According to the Turkish disaster regulations, a shear reinforcement sufficient reinforced concrete beam, a shear reinforcement insufficient beam reinforced concrete beam, and strengthened with GFRP three shear reinforcement insufficient reinforced concrete beam, modeled with the ABAQUS/CAE program.

##### 4.1 The finite element program ABAQUS/CAE

ABAQUS/CAE is a computer-aided engineering software which is capable of nonlinear finite element analysis. This program was used to solve the engineering problems which were created three-dimensional solid models. The creation of the models, analysis of the program's implementation rankings were as follows.

##### 4.1.1 Creating parts of geometry own model

The first step to be made of the beams to be modeled was to create the geometry of the parts belonging to the model. The ABAQUS/CAE (2012), finite element program allows you to create these geometries on your own platform. In this study geometry were built with ABAQUS/CAE program. The geometries of the concrete specimens, reinforcement, GFRP strip and anchorage elements were formed for models of the T-section beam. Solid element type was selected for concrete, and GFRP strip and wire element type was selected for reinforcement and anchorages.

Table 5 The actual values of the parameters used in the analysis

	Density, kg/m <sup>3</sup>	Elasticity Modulus, GPa	Shear Modulus, GPa	Poisson Ratio
Mild Steel	7800	210	76	0,29
Concrete	2400	48	20	0,20
GFRP	1800	26	10	0,28

##### 4.1.2 Introducing the material properties of ABAQUS CAE program

In the study, properties of materials to be used in the next step in the study were defined in the program. The actual values of the parameters used in the analysis were given in Table 5. In the same step, the process of the material properties was carried out in the section of the desired geometry assigning. The proximity of real analysis of models was associated with the introduction of features to the program. Wrapping cases, sample sizes, load status, compressive strength, etc. Properties of concrete materials affect the stress-strain curve. Many mathematical model assumptions were made for stress-strain curve of the concrete material. For these mathematical models, test data on concrete material and behaviors like plastic, elastic etc. were taken into consideration. Concrete Damage Plasticity (CDP) model has been used in the ABAQUS/CAE finite element program for modeling concrete properties and damage behavior (Fig. 5).

Concrete Damage Plasticity is a concrete damage plasticity model for unreinforced or reinforced concrete. This model allows nonlinear analysis of concrete under load conditions. In addition, this model describes the nonlinear behavior of concrete under compression and tensile stress. Stress-strain curves under compressive and tensile stresses of the concrete damage plasticity model were shown in Fig. 5 and Fig. 6.

To check the behavior under compressive and tensile stresses  $d_c$  (compressive damage) and  $d_d$  (tensile damage) stiffness reduction parameters was used. The mathematical value of this parameter was shown at Eq. (1).

$$E_0(1-d_t,c)E_0 \tag{1}$$

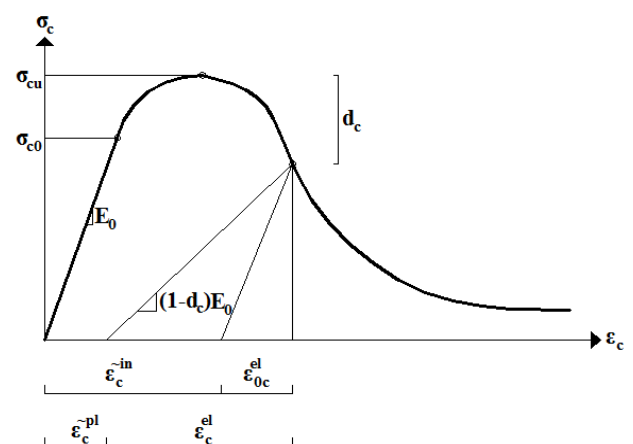


Fig. 5 Concrete Damage Plasticity model stress-strain curve under compressive stress (Hibbitt *et al.* 2011)

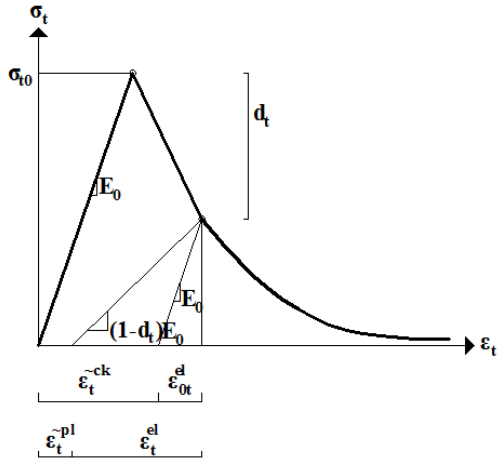


Fig. 6 Concrete Damage Plasticity model stress-strain curve under tension, stress (Hibbitt *et al.* 2011)

If  $d=0$   $E_0$  will be  $E$  and modulus of elasticity will belong to the elastic region.

If  $d=1$  then the value will be undefined.

In the range of  $0 < d < 1$ , it was trying to define nonlinear behavior by changing  $d_c$  and  $d_t$  stiffness reduction parameters. In addition, for this model program was required to define the value of expansion angle, eccentricity, compressive and tensile from the meridian, viscosity parameter, the biaxial compressive strength of concrete, the tensile strength ratio. Concrete material data were obtained from uniaxial compressive, and tensile stress-strain test results data. Inelastic deformation values caused by pressure and shrinkage shown in Eq. (2) and Eq. (3) (Hibbitt *et al.* 2011).

$$\varepsilon_c^{in} = \varepsilon_c - \frac{\sigma_c}{E_0} \quad (2)$$

$$\varepsilon_t^{ck} = \varepsilon_t - \frac{\sigma_t}{E_0} \quad (3)$$

By using inelastic deformation values obtained from Eq. (2) and Eq. (3) and  $d_c$  and  $d_d$  stiffness reduction parameters, plastic strain values caused by compressive and tension were calculated according to the formula as shown in Eq. (4) and Eq. (5). ABAQUS Concrete Damage Plasticity model of the data was entered to the concrete compression damage and concrete tension damage tables (Hibbitt *et al.* 2011).

$$\varepsilon_c^{pl} = \varepsilon_c^{in} - \frac{d_c}{1-d_c} * \frac{\sigma_c}{E_0} \quad (4)$$

$$\varepsilon_t^{pl} = \varepsilon_t^{ck} - \frac{d_t}{1-d_t} * \frac{\sigma_t}{E_0} \quad (5)$$

While Concrete Damage Plasticity model, creating values was obtained from Standard Design of Concrete Structures (TS EN 1992-1-1/April 2009) and Standard Rules Applied in Buildings (EUROCODE 2 2008). Classical Metal Plasticity (CMP model was used for the elastic and plastic material characteristic of reinforcing steel, and anchorages. The plastic behavior of a material was defined by the yield point and after. It takes place transition from elastic to plastic behavior from the yield point in the stress-strain curve. The nominal stress-strain

values are obtained using the test data. There was a real stress-strain values by using nominal stress-strain values.

In ABAQUS/CAE finite element program, while plasticity data defining, real stress value Eq. (6) and the real value of plastic deformation change Eq. (7) are used (Ellobody *et al.* 2014).

$$\sigma_{true} = \sigma * (1 + \varepsilon) \quad (6)$$

$$\varepsilon_{true}^{pl} = \ln(1 + \varepsilon) - \frac{\sigma_{true}}{E_0} \quad (7)$$

#### 4.1.3 Making the assembly of created parts

The formed parts were assembled together by assembling them together. The step of forming the parts of a Model was shown in Fig. 6.

#### 4.1.4 Creation of the analysis type and analysis step

In the ABAQUS / CAE finite element program, Static General analysis type was selected. Then, the values of the analysis steps were created.

#### 4.1.5 Parts identification of cross-contact

In this step, the contact states of the assembled parts with each other were modeled. Concrete-reinforcement, and concrete-anchorage contact surface were chosen as Embedded Region. The concrete contact surface with GFRP strips was defined as Tie.

#### 4.1.6 Load and boundary defining the terms

The assignment of the loads belonging to the model, and the definition of the boundary conditions, were carried out by the Load step. The load was applied step by step as a singular load as it was applied to modelled beams in experiments (Fig. 3).

#### 4.1.7 Divided by finite elements model

As the most important and distinctive feature of the finite element method, dividing the body finite element meshes provided by the Mesh step in ABAQUS/CAE program. Mesh operation was carried out separately for each part. 3D Stress was selected for concrete and GFRP elements, Truss was selected for reinforcement and anchorages elements. Mesh range was obtained 0,1 for concrete, 0,08 for reinforcement and anchorage and 0,02 for GFRP. As interest in the results of the analysis of material properties the division of the finite element model was also very important with regular and frequent mesh range. The mesh of a model was shown in Fig. 7.

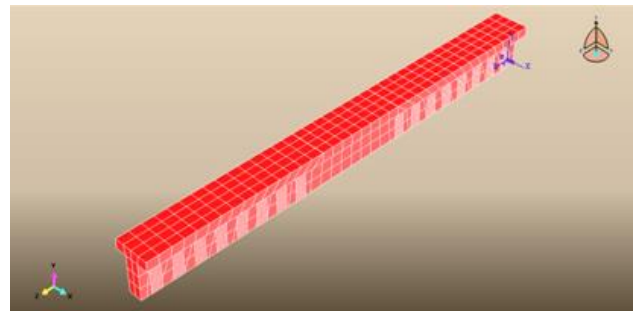


Fig. 7 Mesh of the beams

Table 6 Comparison of the analysis and test results

Specimen name	Test specimens load capacity (kN)	Test specimens maximum displacement (mm)	Analytical models load capacity (kN)	Analytical models maximum displacement (mm)
DE1	185,96	25,42	185,96	23,02
DE2	138,76	22,07	120,17	30,07
DE3	169,08	28,23	169,08	23,12
DE4	174,94	28,45	174,94	24,22
DE5	185,30	25,44	185,30	25,01

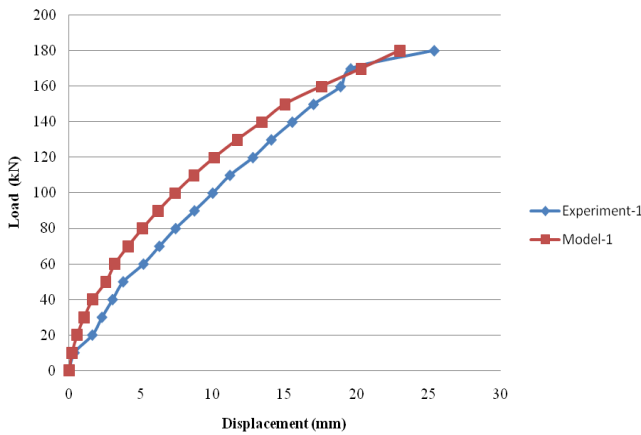


Fig. 9 Experiment-1 and Model-1 load-displacement graph

4.1.8 The initialization of analysis

After the analysis was complete, the results of analysis of the model are displayed in the results table. Model of graphs were drawn with Create XY Data command in the Visualization step. Node numbers are indicated while these graphs are being drawn. Before the load-time graph, then the displacement-time graph was plotted with Create XY Data/ODB field output command. It has passed the chart to the load-displacement curves by using Create XY Data/Operate on XY Data command.

5. Comparison test and analysis results

Comparison of the test and analytical results of the strengthened reinforced concrete beams were given in Table 6, Fig. 8, Fig. 9, Fig. 10, Fig. 11, and Fig. 12. It was seen from the result, in Model-2, the rate of increase of displacement was higher than the increase of load rate. Moreover, in Model-1 and Model-5 displacement was lower than DE1 and DE5 test specimens displacements. It was seen, finite element based ABAQUS program is inadequate in the modeling of the reinforced concrete specimens under shear force.

In Fig. 9, the analysis results and the test results of the model with sufficient strength against shear are compared. In this case, the bending reinforcement yielded at 180,24 kN. In the same case, the midpoint displacement of the beam at the bending reinforcement was 25,42 mm. The displacement value of the model-1 at the same load was determined as 23,02 mm. DE1 test specimen did 2,4 mm

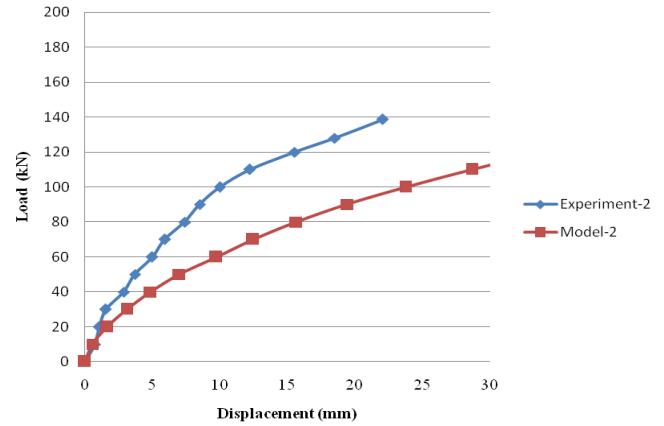


Fig. 10 Experiment-2 and Model-2 load-displacement graph

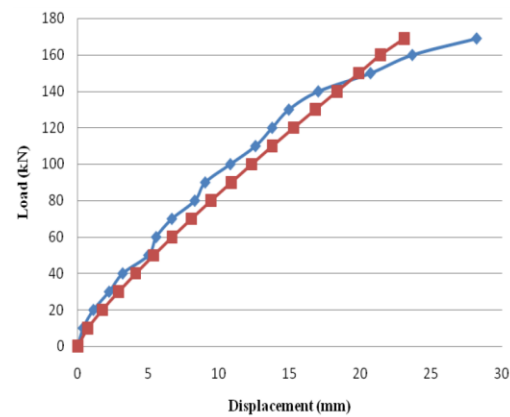


Fig. 11 Experiment-3 and Model-3 load-displacement graph

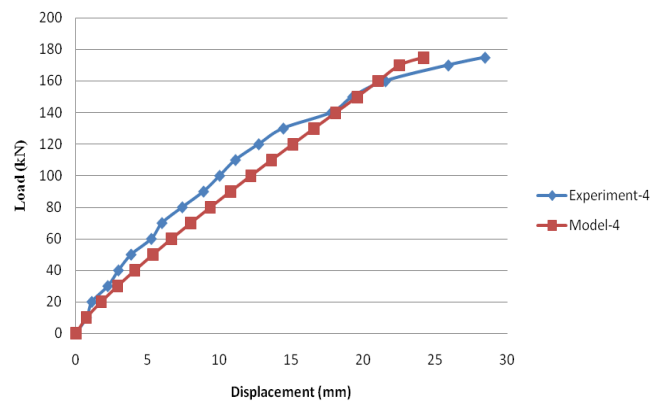


Fig. 12 Experiment-4 and Model-4 load-displacement graph

displacement more than Model-1.

In Fig. 10, the analysis results and the test results of the model with insufficient strength against shear are compared. In Specimen-2, although the test results and analytical model have similar results for small loads, the difference between the displacement values increased as the load increased. Experiment 2 collapsed at 138,76 kN with a displacement of 22,07 mm at this load, but the Model-2 displaced this displacement at a lower load than this load. In the analytical modeling of this test specimen, the analytical

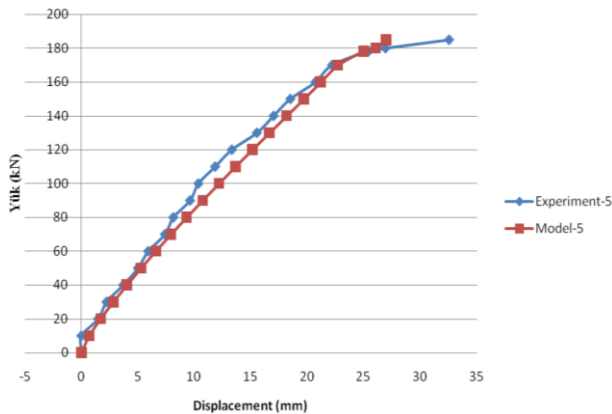


Fig. 13 Experiment-5 and Model-5 load-displacement graph

element converged under a lower load and could not reach the maximum load level carried by the test specimen. DE2 test specimen did 8 mm less than Model-2 displacement.

Fig. 11 shows the results of strengthening with GFRP strips against shear crack by using 2 anchorages and approximately equal results were obtained from the model and the experiments. In Specimen 3, the displacement value of 169,08 kN displacement load is 28,23 mm while the displacement value of the same load for Model-3 is 23,12 mm. DE3 test specimen did 5,13 mm displacement more than Model-3 displacement.

Fig. 12 shows that the model and test results strengthened with GFRP strips against 3 anchorages were close to each other. The load value of the Specimen 4 was 174,94 kN displacement was determined as 28,45 mm, and the displacement value of the same load for Model-4 was determined as 24,22 mm. DE4 test specimen did 4,23 mm displacement more than Model-4 displacement.

Fig. 13 shows that the model was strengthened with GFRP strips against shear crack with 4 anchorages and close values are found the test results. The displacement value of the yield load of 178,28 kN in Specimen-5 results was 25,44 mm while the displacement value for the same load of Model-5 is 25,01 mm, DE5 test specimen did 0,43 mm displacement more than Model-5 displacement.

In the studies, the analytical model prepared according to the results obtained from the experimental work is applied to different loads, and the analytical results are compared with the experimental results. If the results obtained from the experiment, and the results obtained from the analytical element are compatible, it is assumed that the analytical model is formed correctly. The results obtained from different loads applied to the analytical element that is correctly modeled are assumed to be obtained from the same load applied test specimen.

The maximum load applied to the analytical model is the maximum load carried by the test specimens. Therefore, the deformations that occur at these loads applied to the analytical elements have been identified and compared. Excessive load on the maximum load carried by the test specimens to the analytical elements and trying to displacement under this load will go beyond the scope of the study.

## 6. Conclusions

When the analytical results of the GFRP reinforced beams are compared with the analytical results, at the maximum load level, the shear reinforcement showed a displacement of the adequate test specimen at the center of the beam and the displacement determined at the center of the beam of the analytical model by 9,44%. The displacement of the beam center at the maximum load level of the analytical model of this specimen differs by 18,77% from the experimental specimen using 2 anchorages from the reinforced test specimens. The displacement of the center of the beam at the maximum load level of the analytical model of this specimen varied by 14,87% with the experimental specimen strengthened using 3 anchorages. The displacement of the beam center at the maximum load level of the analytical model of this specimen differs by 1,69% from the experimental specimen using 4 anchorages from the reinforced test specimens. The shear reinforcement showed that the displacement of the inadequate test specimen in the center of the beam and the displacement determined in the center of the beam of the analytical model by 26,60 %.

In the analytical modeling of an inadequate test specimen, the difference between the displacement in the middle of the opening of the test specimen and the displacement in the middle of the opening of the analytical model is very large. However, the results obtained from the analysis of analytical models of other test specimens are quite successful.

## 7. Suggestions

In this study, the load-displacement graphs of experiments and models were compared with each other. From these results obtained by entering the elastic and plastic values for concrete and reinforcement into the ABAQUS/CAE finite element program of linear elastic values of GFRP and anchorage material, maximum mesh span was defined in the study. Increasing the mesh size has increased the zooming of the results. It is considered that the analysis results of beam models will come closer to the reality if mesh spacing is chosen less.

It is considered that the plastic values obtained by laboratory results of GFRP materials used in the experiments will be determined and the results will be closer to reality by introducing the program.

Experimental and analytical investigation of the effect of GFRP strips at different widths, thickness and spacing, with the shear strength of the beams, is proposed. Moreover, it is recommended to use different anchor diameter.

It is considered that the analysis results of beam models will come closer to reality if the mesh spacing is most frequently selected in the ABAQUS/CAE finite element program of linear elastic values of GFRP and anchor materials.

Properties of Concrete Damage Plasticity, and Classical Metal Plasticity models used for concrete and reinforcement should be investigated by using different models.

This study does not make much contribution to the

development of the finite element method. When the specimen sizes are large, and the experiment costs are high, a few test specimens can be modelled with finite element based ABAQUS etc. Later, instead of producing and testing large number of test specimens, the load, geometry, etc. variables can be applied to analytical models.

## References

- AASHTO (1998), Load Resistance and Factor Design Bridge Design Specifications, SI Units, Second Edition, American Association of State Highway Transportation, Offices, Washington, DC.
- ABAQUS/Standard User's Manuals (2002), Version 6.3, Hibbit, Karlsson and Sorensen, Inc., USA.
- Ahmed, A. (2014), "Modelling of reinforced concrete beam subjected to impact, vibration using ABAQUS", *Int. J. Civil Struct. Eng.*, **4**(3), 227.
- Baskar, K., Shanmugam, N.E. and Thevendran, V. (2002), "Finite-element analysis of steel-concrete composite plate girder", *J. Struct. Eng.*, **128**(9), 1158-1168.
- Bath, E.K. and Wu, H. (2006), "Efficient nonlinear finite element modeling of slab on steel stringer bridges", *Finite Elem. Anal. Des.*, **42**, 1304-1313.
- CEB (1983), Application of the Finite Element Method for Two-Dimensional Reinforced Concrete Structures, Bulletin No. 159, CEB-FIP.
- DBYBHY (2007), Regulation of Buildings to be Built in Earthquake Regions, Turkish Standards Institute, Ankara.
- Demir, A., Caglar, N., Ozturk, H. and Sumer, Y. (2016), "Nonlinear finite element study on the improvement of shear capacity in reinforced concrete T-Section beams by an alternative diagonal shear reinforcement", *Eng. Struct.*, **120**, 158-165.
- Dogan, A.B. and Anil, O. (2010), "Nonlinear finite element analysis of effective CFRP bonding length and strain distribution along concrete-CFRP interface", *Comput. Concrete*, **7**(5), 437-453.
- Domínguez, E., Tena-Colunga, A. and Gelacio Juárez-Luna, G. (2015), "Nonlinear finite element modeling of reinforced concrete haunched beams designed to develop a shear failure", *Eng. Struct.*, **105**, 99-122.
- Ellobody, E., Feng, R. and Ve Young, B. (2014), *Finite Element Analysis and Design of Metal Structures*, Butterworth-Heinemann, Elsevier.
- EUROCODE 2 (2008), Standard Rules Applied in Buildings.
- Fu, K.C. and Lu, F. (2003), "Nonlinear finite-element analysis for highway bridge superstructures", *J. Bridge Eng.*, **8**(3), 173-179.
- Gilbert, R.I. and Warner, R.F. (1978), "Tension stiffening in reinforced concrete slabs", *J. Struct. Div.*, **104**(ST12), 1885-1900.
- Gupta, A.K. and Maestrini, S.R. (1990), "Tension-stiffening model for reinforced concrete rebars", *J. Struct. Eng.*, **116**(3), 769-790.
- Hall, J.C. and Kostem, C.N. (1980), "Inelastic analysis of steel multigirder highway bridges", Fritz Engineering Lab Report No. 435.1, Lehigh University, PA, USA.
- Hawileh, R.A. (2012), "Nonlinear finite element modeling of RC beams strengthened with NSM FRP rods", *Constr. Build. Mater.*, **27**, 461-71.
- Helba, A. and Kennedy, J.B. (1995), "Skew composite bridges-analysis of ultimate load", *Can. J. Civil Eng.*, **22**, 1092-1103.
- Hibbit, H., Karlsson, B. and Sorensen, P. (2011), Abaqus Analysis Users Manual, Version 6.11, Dassault Systèmes Simulia Corp., Providence, RI, USA.
- Ibrahimbegovic, A., Boulkertous, A., Davenne, L. and Brancherie, D. (2010), "Modelling of reinforced-concrete structures, providing a crack-spacing based on X-FEM, ED-FEM and novel operator split solution procedure", *Int. J. Numer. Meth. Eng.*, **83**(4), 452-481.
- Kmiecik, P. and Kaminski, M. (2011), "Modelling of reinforced concrete structures and composite structures with concrete strength degradation taken into consideration", *Arch. Civil Mech. Eng.*, **11**(3), 625-636.
- Kotsovou, G.M. and Kotsovos, G.M. (2016), "Behavior of RC Beams with non-bonded flexural reinforced: A numerical experiment", *Comput. Concrete*, **18**(2), 165-178.
- Larbi, A.S., Agbossou, A. and Hamelin, P. (2013), "Experimental and numerical investigations about textile-reinforced concrete and hybrid solutions for repairing and/or strengthening reinforced concrete beams", *Compos. Struct.*, **99**, 152-162.
- Lee, D.H., Hwang, J.H., Ju, H. and Kim, K.S. (2014), "The application of direct tension force transfer model with modified fixed-angle softened-truss model to finite element analysis of steel fiber-reinforced concrete members subjected to shear", *Comput. Concrete*, **13**(1), 49-70.
- Lin, J.J., Fafard, M., Beaulieu, D. and Massicotte, B. (1991), "Nonlinear analysis of composite bridges by the finite element method", *Comput. Struct.*, **40**(5), 1151-1167.
- Mahmud, G.H., Yang, Z. and Hassan, A.M.T. (2013), "Experimental and numerical studies of size effects of Ultra High Performance Steel Fiber Reinforced Concrete (UHPFRC) beams", *Constr. Build. Mater.*, **48**, 1027-1034.
- Nistico, N., Ozbolt, J. and Polimanti, G. (2016), "Modeling of reinforced concrete beams strengthened in shear with CFRP: Microplane-based approach", *Compos. Part B*, **90**, 351-364.
- Razaqpur, A.G. and Nofal, M. (1990), "Analytical model of nonlinear behavior of composite bridges", *J. Struct. Eng.*, **116**(6), 1715-1733.
- Ruano, G., Isla, F., Sfer, D. and Luccioni, B. (2015), "Numerical modeling of reinforced concrete beams repaired and strengthened with SFRC", *Eng. Struct.*, **86**, 168-181.
- Silva, M.F.A. and Haach, V.G. (2016), "A parametric study of the behavior of exterior unreinforced concrete beam-column joints through numerical modeling", *Comput. Concrete*, **18**(2), 215-233.
- Solomon, S.M., El-Salakawy, E. and Benmokrane, B. (2010), "Flexural behavior of concrete beams strengthened with near surface mounted fiber reinforced polymer bars", *Can. J. Civil Eng.*, **37**(10), 1371-1382.
- Stramandinoli, R. and La Rovere, H.L. (2012), "FE model for nonlinear analysis of reinforced concrete beams considering shear deformation", *Eng. Struct.*, **35**, 244-253.
- Thevendran, V., Chen, S., Shanmugam, N.E. and Liew, J.Y.R. (1999), "Nonlinear analysis of steel-concrete composite beams curved in plan", *Finite Elem. Anal. Des.*, **32**, 125-139.
- TS EN 1992-1-1/April (2009), Standard Design of Concrete Structures, Turkish Standards Institute, Ankara, Turkey.
- Wegmuller, A.W. (1977), "Overload behavior of composite steel-concrete bridges", *J. Struct. Div.*, **103**(ST9), 1799-1819.
- Xu, J., Wu, C., Li, Z. and Ching, C.T. (2015), "Numerical analysis of shear transfer across an initially uncrack reinforced concrete member", *Eng. Struct.*, **102**, 296-309.
- Yaman, C. (2015). "Analytical modeling of the effect of anchors on strengthening reinforced concrete beams with glass fiber plates", Master Thesis, Aksaray University, Aksaray, Turkey.
- Zivaljic, N., Nikolic, Z. and Smoljanovic, H. (2014), "Computational aspects of the combined finite discrete element method in modelling of plane reinforced concrete structures", *Eng. Fract. Mech.*, **131**, 669-686.